

## Exotic nuclear phases in the inner crust of neutron stars in the light of Skyrme-Hartree-Fock theory

P. Magierski<sup>a\*</sup>, A. Bulgac<sup>b</sup> and P.-H. Heenen<sup>c</sup>

<sup>a</sup>Faculty of Physics, Warsaw University of Technology,  
ul. Koszykowa 75, 00-662 Warsaw, Poland

<sup>b</sup>Department of Physics, University of Washington,  
Seattle, WA 98195-1560, USA

<sup>c</sup>Service de Physique Nucléaire Théorique,  
U.L.B - C.P. 229, B 1050 Brussels, Belgium.

The bottom part of the neutron star crust is investigated using the Skyrme-Hartree-Fock approach with the Coulomb interaction treated beyond the Wigner-Seitz approximation. A variety of nuclear phases is found to coexist in this region. Their stability and relative energies are governed by the Coulomb, surface and shell energies. We have also found that a substantial contribution is coming from the spin-orbit interaction.

The crust of a neutron star with a typical mass of  $1.4 M_{\odot}$ , contains only 1.2% of the total stellar mass. Nevertheless its structure is important for understanding of several observational issues and thus provides a motivation for theoretical studies (see e.g. [ 1, 2, 3, 4, 5, 6, 7, 8, 9, 10, 11] and references therein).

According to various theoretical models in the inner part of the crust, due to high density and pressure, the nuclei forming a crystalline lattice are immersed in a neutron gas. The electrons at these densities are ultrarelativistic particles and are assumed to form a uniform background.

In the bottom part of the inner crust the interplay between the Coulomb and the surface energies leads to the appearance of various nuclear phases, characterized by different shapes. The early predictions, based on the liquid drop or Thomas-Fermi models, with quite restrictive symmetry conditions, lead to the considerations of five phases, formed in the region where the nucleon density varies from  $0.03$  to  $0.1 \text{ fm}^{-3}$ . These are: spherical nuclei, rods (“spaghetti” phase), slabs (“lasagna” phase), tubes and bubbles (see [ 7] and references therein).

These approaches however provided an oversimplified description of the system. First, due to the Wigner-Seitz approximation which has been used, there is no distinction between phases resulting from different lattice geometries, second, the quantum effect as-

---

\*This research was supported in part by the Polish Committee for Scientific Research (KBN) under Contract No. 5 P03B 014 21 and the Wallonie/Brussels-Poland integrated action program. Numerical calculations were performed at the Interdisciplinary Centre for Mathematical and Computational Modelling (ICM) at Warsaw University.

sociated with the shell correction energy has been neglected, and last but not least, the symmetry conditions, which admit only spherical, cylindrical and planar structures, are not sufficient to describe properly the variety of nuclear shapes present in the crust.

Our approach, which is free from the aforementioned limitations, can shed some light on the complexity of the inner crust structure. The ground and excited (isomeric) states of neutron-proton-electron (*npe*) matter have been determined by the Skyrme-Hartree-Fock method. We have solved the HF equations by discretization in coordinate space, within a cubic box and with periodic boundary conditions imposed on the nucleon wave functions [12]. The details of this approach have been described in Ref.[10].

In the HF approximation, the total energy of a nuclear system is, in general, a functional of three local densities: total nucleon density  $\rho(\mathbf{r}) = \rho_p(\mathbf{r}) + \rho_n(\mathbf{r})$ , total kinetic density  $\tau(\mathbf{r}) = \tau_p(\mathbf{r}) + \tau_n(\mathbf{r})$  and total spin-orbit density  $\mathbf{J}(\mathbf{r}) = \mathbf{J}_p(\mathbf{r}) + \mathbf{J}_n(\mathbf{r})$ . Each of the densities is in turn expressed through the single-particle wave functions  $\phi_i^q(\mathbf{r}, \sigma)$ :

$$\rho_q(\mathbf{r}) = \sum_{i,\sigma} n_i^q |\phi_i^q(\mathbf{r}, \sigma)|^2, \quad (1)$$

$$\tau_q(\mathbf{r}) = \sum_{i,\sigma} n_i^q |\nabla \phi_i^q(\mathbf{r}, \sigma)|^2, \quad (2)$$

$$\mathbf{J}_q(\mathbf{r}) = -i \sum_{i,\sigma,\sigma'} n_i^q \phi_i^{q*}(\mathbf{r}, \sigma) \nabla \phi_i^q(\mathbf{r}, \sigma') \times \langle \sigma | \boldsymbol{\sigma} | \sigma' \rangle \quad (q = n,p), \quad (3)$$

where  $\frac{1}{2}\sigma$  ( $\sigma = \pm 1$ ) is the spin projection on the  $z$ -axis, and  $n_i^q$  is the occupation factor, which is 1 below the Fermi level and zero otherwise.

The Skyrme energy functional can be written as:

$$\begin{aligned} E_{sk} = & \int \left[ \frac{\hbar^2}{2m} \tau + B_1 \rho^2 + B_2 (\rho_p^2 + \rho_n^2) + B_3 \rho \tau + B_4 (\rho_p \tau_p + \rho_n \tau_n) + \right. \\ & + B_5 \rho \nabla^2 \rho + B_6 (\rho_p \nabla^2 \rho_p + \rho_n \nabla^2 \rho_n) + B_7 \rho^{2+\gamma} + \\ & \left. + B_8 \rho^\gamma (\rho_p^2 + \rho_n^2) + B_9 (\rho \nabla \cdot \mathbf{J} + \rho_p \nabla \cdot \mathbf{J}_p + \rho_n \nabla \cdot \mathbf{J}_n) \right] d^3r. \end{aligned} \quad (4)$$

The coefficients  $B_i$  depend on the Skyrme force parameters [12]. It is useful to distinguish the following contributions to the Skyrme energy functional:

$$E_{sksurf} = \int (B_5 \rho \nabla^2 \rho + B_6 (\rho_p \nabla^2 \rho_p + \rho_n \nabla^2 \rho_n)) d^3r, \quad (5)$$

$$E_{so} = \int (B_9 (\rho \nabla \cdot \mathbf{J} + \rho_p \nabla \cdot \mathbf{J}_p + \rho_n \nabla \cdot \mathbf{J}_n)) d^3r, \quad (6)$$

where  $E_{sksurf}$  contains the contribution to the surface energy and  $E_{so}$  is the spin-orbit term.

For a correct description of *npe* matter one has to add to the Skyrme energy functional the Coulomb term and the kinetic energy of electrons:

$$E = E_{sk} + E_{Coul} + E_{el}, \quad (7)$$

where the direct Coulomb energy has been calculated by solving the Poisson equation with periodic boundary conditions. The Coulomb exchange term for both protons and electrons has been treated in the Slater approximation.

Typical results for two values of the average total density  $\rho_{av} = \frac{1}{V} \int_V (\rho_p + \rho_n) d^3r$ , and the proton-to-nucleon ratio ( $Z/A$ ) ensuring the  $\beta$  stability condition, are shown in Fig. 1. The total energy densities have been plotted with respect to the value of the spherical system  $Q_p = 0$ .

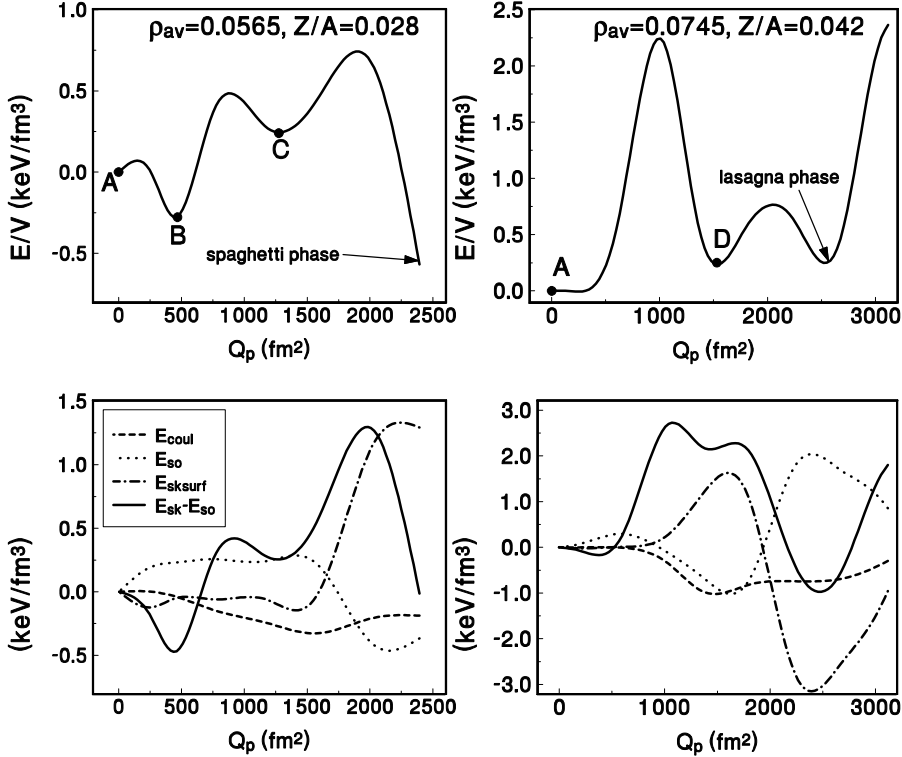


Figure 1. The results of the Skyrme-Hartree-Fock calculations (using SLy4 force) presented as a function of the axial proton quadrupole moment:  $Q_{20} = Q_p$ . The calculations have been performed in a box of lengths:  $d = 26 fm$  (left panel) and  $d = 20.8 fm$  (right panel). The upper subfigures show the total energy density and the lower subfigures the contribution to the total energy coming from various terms in the density functional (see text for details). The phase A consists of spherical nuclei in the scc lattice, the phases B and C denote the scc geometries differing by the nuclear deformations. The D phase corresponds to the bcc lattice.

The energy density has several local minima, corresponding to various nuclear shape and lattice geometries. It was shown in Ref.[ 10] that the relative position of various nuclear configurations is a sensitive function of the density. It is a consequence of the

shell effects associated with unbound neutrons [ 13]. Hence different nuclear phases may coexist in the same density range. There is an obvious larger variety of nuclear shapes than it was predicted in the previous approaches ([ 7, 9] and references therein).

In the lower subfigures of Fig. 1, the contributions from the Coulomb energy, the  $E_{sksurf}$  term and the spin-orbit term, have been shown. One can make the following observations:

- The Coulomb energy decreases as a function of  $Q_p$  for small values of quadrupole moment and then increases slightly for large  $Q_p$  values. This is related to the fact that large  $Q_p$  values correspond to the configuration where the nuclei from neighboring cells join each other. Hence the configuration favored by the Coulomb interaction consists of deformed nuclei, but not necessarily in the shape of rods or slabs.
- The part of the surface energy coming from the  $E_{sksurf}$  term follow approximately the behavior of the term  $E_{sk} - E_{so}$ . It suggests that the surface energy dominates the behavior of  $E_{sk}$  as a function of the deformation.
- The amplitude of variation of the spin-orbit term  $E_{so}$  is of the same order as the  $E_{sk} - E_{so}$ . The spin-orbit energy is a sensitive function of  $Q_p$  and clearly have a direct influence on the appearance and depths of local minima of the total energy curve. One has to remember that this term gives the substantial contribution to the shell energy.

Finally one has to mention that the pairing correlation were not included in the above calculations. The pairing would smooth the total energy curve and thus its role in the inner edge of the neutron star crust needs a thorough examination.

## REFERENCES

1. G. Baym, H.A. Bethe, C.J. Pethick, Nucl. Phys. **A175** (1971) 225.
2. J.W. Negele and D. Vautherin, Nucl. Phys. **A207**, (1973) 298; P. Bonche and D. Vautherin, Nucl. Phys. **A372** (1981) 496; Astron. Astrophys. **112** (1982) 268.
3. J.M. Lattimer, C.J. Pethick, D.G. Ravenhall, Nucl. Phys. **A432** (1985) 646.
4. R.D. Wilson and S.E. Koonin, Nucl. Phys. **A435** (1985) 844.
5. M. Lassaut, H. Flocard, P. Bonche, P.-H. Heenen, E. Suraud, Astron. Astrophys. **183** (1987) L3.
6. K. Oyamatsu, Nucl. Phys. **A561** (1993) 431.
7. C.J. Pethick and D.G. Ravenhall, Annu. Rev. Nucl. Part. Sci. **45** (1995) 429.
8. F. Douchin, P. Haensel, J. Meyer, Nucl. Phys. **A 665** (2000) 419.
9. F. Douchin, P. Haensel, Phys. Lett. **B485** (2000) 107.
10. P. Magierski, P-H. Heenen, Phys. Rev. **C65** (2002) 045804.
11. P. Magierski, A. Bulgac, P.-H. Heenen, Int. J. Mod. Phys. **A17** (2002) 1059.
12. P. Bonche, H. Flocard, P.-H. Heenen, S.J. Krieger, M.S. Weiss, Nucl. Phys. **A443** (1985) 39.
13. A. Bulgac, P. Magierski, Nucl. Phys. **A683** (2001) 695; Phys. Scripta **T90** (2001) 150; Acta Phys. Pol. **B32** (2001) 1099.